15

Using CDMA as Anti-Collision Method for RFID - Research & Applications

Andreas Loeffler
Friedrich-Alexander-University of Erlangen-Nuremberg
Germany

1. Introduction

The increasing number of deployed RFID systems and the resulting need for fast recognition of a given amount of RFID tags puts great demand on future RFID readers. Applications requesting for a fast capture of RFID tags are mainly found in logistic and manufacturing processes. Imagine trucks driving through large RFID gates, where each RFID tagged package or even item has to be identified. Also, fast production with tagged units approaching in quick succession would need a fast recognition of RFID tags. Therefore, if several tags are located within the range of a reader, signals from some of these tags will clash. For this very reason anti-collision procedures are widely deployed to prevent tags from broadcasting their information simultaneously. Existing RFID multiple access solutions for the uplink channel are based on Time Division Multiple Access (TDMA). Fig. 1 shows the TDMA method, pointing out that the tags in the reader's field transmit their data at different moments in time (slots) (Finkenzeller, 2003).
As may be imagined, the application of TDMA in RFID systems ensures that each RFID tag in range will be detected on condition that the amount of time available is sufficient. If this condition is false, the system comes to hard decisions, so that, finally, not every tag in range has been recognized successfully. Therefore, the usage of TDMA methods pushes the

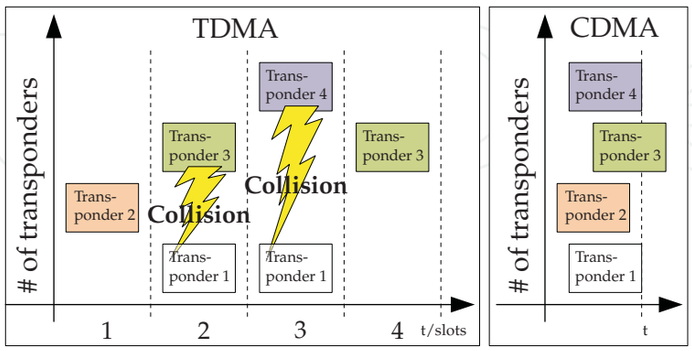

Fig. 1. Comparison of TDMA and CDMA communication channel access techniques for RFID

envelope of the system when a very high number of tags have to be scanned within a given time span.
"Graceful degradation". This quotation from Aein (1964) describes very well the behavior of Code Division Multiple Access (CDMA). In comparison to TDMA with its "hard decisions",

CDMA-based systems take “soft decisions”, which means, that within the system each additionally introduced RFID tag decreases the overall probability of detection of all tags. However, for a particular amount of tags, the system may be optimized in such a way that the time needed for detection may be minimized. Therefore, for an RFID system under those certain circumstances, the introduction of CDMA may offer a way out (Fig. 1). The transponders, each equipped with a unique quasi-orthogonal spreading code (e.g., Gold codes (Gold, 1967a)), may use the radio channel whenever the transponders are ready to transmit their data (asynchronous CDMA). The objective is the realization of a DS (direct sequence)-CDMA-based RFID system using semi-passive UHF transponders, with the reader providing the recognition of multiple transponders simultaneously. This means that the transponders are transmitting data within the same time range and frequency band, in contrast to the existing systems based on TDMA.
The realized UHF transponders operate in semi-passive mode, meaning that the digital part of the transponder, i.e., the data generation, has an active power supply, whereas the high frequency (HF) part works in passive mode taking advantage of the backscatter principle.
The attendant RFID reader, though, is separated into two parts. Part one, described as transmitting system, generates a carrier wave at around 867 MHz. Part two, the receiving system, mainly demodulates the incoming backscattered signals of the RFID tags.
This chapter is organized in seven sections. The first section gives a brief introduction to the topic of anti-collision in UHF-RFID-based systems. The following sections introduce CDMA by outlining the advantages over the current used TDMA schemes. After introducing particular problems backscattering RFID systems have to deal with, a concept and an implementation of such a CDMA-based RFID system is shown. The chapter ends with various measurements concerning the system and subsequent results.

2. Anti-collision: EPC class 1 Gen 2

This section outlines some basic issues regarding anti-collision methods within RFID. Basic and state-of-the-art anti-collision methods are shown in Subsection 2.1. Subsection 2.2 presents theoretical performance issues regarding the throughput by comparing state-of-the-art TDMA methods with CDMA anti-collision methods.

2.1 ALOHA and slotted ALOHA

Before elucidating the state-of-the-art anti-collision method for UHF RFID systems, the principle of ALOHA and unslotted ALOHA (Bertsekas & Gallager, 1992) is illustrated, as the principle of ALOHA provides the basis for the modern anti-collision protocols. The ALOHA protocol (or pure ALOHA), first published by Abramson (1970), is a very simple transmission protocol. The transmitter sends its data, no matter if the transmission channel is free or not. This means the transmitter does not care about collisions with other transmitters. The transmitter resends its data later, if the acknowledgment from the receiver is missing. RFID systems based on the principle of pure ALOHA are, e.g., based on the TTF principle, i.e., transponder-talks-first. The IPX protocol from IPICO (2009) is an example for RFID systems using unslotted or pure ALOHA.
An extension of the ALOHA protocol, called slotted ALOHA (Roberts, 1975) introduces time slots in which the transmitter must send its data at the beginning. Therefore, collisions only occur within a full time slot. This extension doubles the maximum throughput of the system. Most current RFID protocols are based on the principle of slotted ALOHA, as is also the very commonly used EPC standard UHF Class-1 Generation-2 air interface protocol

V1.2.0 (ISO 18000-6C), commonly known as "Gen2". Basically, the "Gen2" standard defines, that every communication is triggered by the RFID reader, i.e., RTF (reader-talks-first). An inventory round, i.e., the process of detecting all available transponders, is started with the *Query*-command to acquire all transponders available in the read range. This command inherits a so called Q-parameter. Using this Q-parameter, every transponder generates a random number RN in the range $[0; 2^Q - 1]$ and initializes its internal slot counter with this random number. If, at a given moment, the value of the slot counter of one or more transponders equals 0, the transponders send a 16 bit random number called RN_{16}. After the acknowledgment of the RN_{16} through the reader, the electronic product code (EPC) is transmitted from the transponder to the reader and the transponder will be marked as *inventoried*. All the left-over (non-marked) transponders are prompted to decrement its slot counter by sending a *QueryRep*-command, and the procedure starts all over again. In the case of several transponders initializing their slot counters with the same random number RN, it will come sooner or later to a signal collision as the slot counters will reach zero at the same time slot. If the reader recognizes such a collision, another inventory round will be initiated to identify the left-over transponders. Therefore, a newly value of Q will be introduced and new random numbers will be calculated. To sum up, one could say that the choice of Q is a typical trade-off. Choosing a high Q will lead to a smaller number of collisions, at the expense of an increasing time needed for an inventory round. Indeed, a smaller Q will lead to less acquisition time, but to more collisions.
Plenty of work has been done to improve the current EPC standard. Improving the current standard anti-collision method by choosing an appropriate value of Q, e.g., dynamically, is described in Maguire & Pappu (2009); Pupunwiwat & Stantic (2010); Wang & Liu (2006). The right choice of Q is of great importance for the overall system performance, so that an accurate estimation would improve the time needed for an inventory round. Slightly new algorithms, based on the current EPC "Gen2" standard are outlined, e.g, in Cui & Zhao (2009); Lee et al. (2008). New better performing algorithms for the slotted ALOHA protocol for RFID are described in Bang et al. (2009); Choi et al. (2007); Liu et al. (2009); Makwimanloy et al. (2009). A complete new system with time hopping on the communication link from tag to reader is outlined in Zhang et al. (2010).

2.2 Comparison: CDMA versus TDMA in UHF-RFID

The throughput S in dependence of the traffic channel rate G describes the performance of a given transmission system regarding how many packets must be transmitted (statistically) until a successful transmission occurs. This statement is given with the term $\frac{G}{S}$ as described by Kleinrock & Tobagi (1975). The reciprocal of this term, i.e., $\frac{S}{G}$ defines accordingly the probability of a successful transmission. The channel capacity is determined by maximizing S with respect to G (Kleinrock & Tobagi, 1975). According to Abramson (1970) the pure ALOHA transmission has a relation between S and G of

$$S = G\,e^{-G} \tag{1}$$

, whereas the throughput of the slotted ALOHA transmission is defined after Roberts (1975) with

$$S = G\,e^{-2G} \tag{2}$$

. Accordingly, the maximum channel capacity is $\frac{1}{2e} \approx 18.4\%$ for pure ALOHA and $\frac{1}{e} \approx 36.8\%$ for slotted ALOHA.
For a fair comparison between CDMA-based systems and ALOHA systems, the total

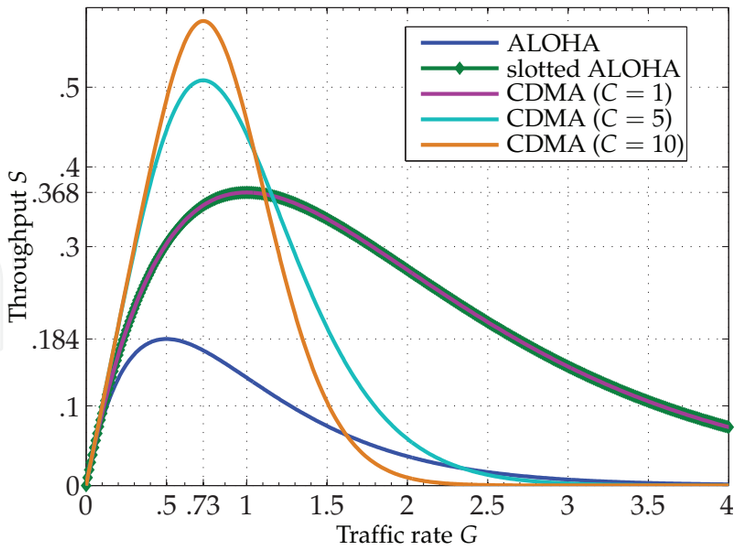

Fig. 2. Various throughputs S over traffic rate G for ALOHA, slotted ALOHA and CDMA

bandwidth has to be maintained the same for both systems. A CDMA system has a so called spreading factor C, which is proportional to the length of the spreading codes respectively the ratio between chip rate and bit rate (i.e., R_{chip}/R_{bit}) used. According to Linnartz & Vvedenskaya (2009) the throughput S and the offered traffic rate G is

$$S = G\, e^{-CG} \sum_{k=0}^{C-1} \frac{(CG)^k}{k!}. \tag{3}$$

Setting $C = 1$ leads to the slotted ALOHA transmission scheme. Figure 2 shows various throughputs S over the traffic rate G. The figure shows the throughputs for ALOHA (channel capacity 18.4%), slotted ALOHA and CDMA with spreading factor $C = 1$ (channel capacity 36.8%), CDMA with $C = 5$ (channel capacity 50.87%) and CDMA with $C = 10$ (channel capacity 58.31%). This graph shows the basic difference between TDMA (ALOHA-based) and CDMA systems. In general, TDMA-based RFID systems can handle much more RFID transponders with a lower overall throughput. CDMA-based system, on the other hand, are able to handle a limited amount of RFID tags with higher overall throughput. For instance, assuming a limited amount of RFID transponders for a traffic rate $G = 0.73$. The throughput of unslotted ALOHA would be $S_{\text{ALOHA}} = 16.95\%$ and the throughput of slotted ALOHA $S_{\text{unslotted ALOHA}} = 35.18\%$. A CDMA-based system with a spreading factor C of 10 would have there its maximum throughput of $S_{\text{CDMA},C=10} = 58.31\%$. This scenario is shown in Figure 2.

Finally, it can be stated that CDMA-based RFID systems may be better for particular applications, in which the number of transponders is limited and the inventory process has to be made very fast, e.g., fast production lines and automation processes.

Particular slotted ALOHA CDMA systems and corresponding performances may be found in Gopalan et al. (2005); Sakata et al. (2007). Other works describe certain CDMA systems with error correction which really outperform the TDMA-based systems. Examples can be found in Liu et al. (2001); Liu & El Zarki (1994); Lo et al. (1996); Sastry (1984); van Nee et al. (1995). Also this list is not complete it gives a short overview of CDMA-based system performances.

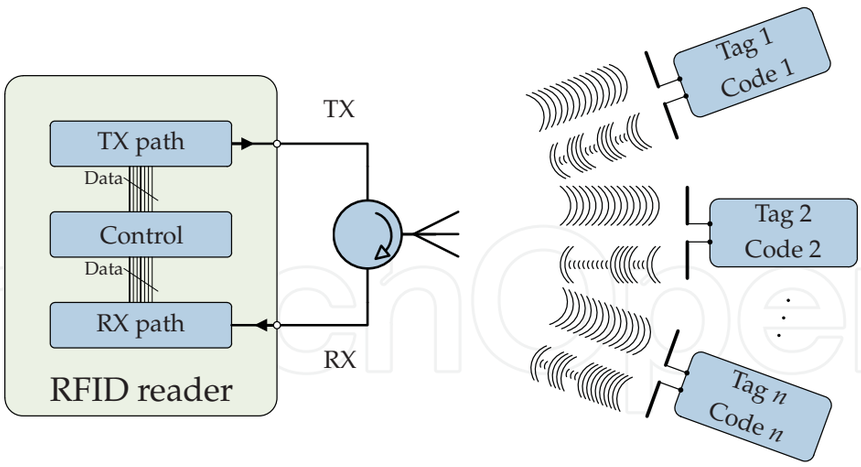

Fig. 3. Basic architecture of RFID system; depicted in monostatic antenna configuration

3. Concept of CDMA-based system

This section presents the basics of the proposed RFID system. Going into more detail, Subsection 4.1 shows the architecture of the Transmitting System (TX system path) followed by Subsection 4.2 presenting the proposed semi-passive RFID transponders and Subsection 4.3 describing the Receiving System (RX system path).
Figure 3 shows the basic architecture of the CDMA-based RFID system. Generally, it consists, as any other RFID system of two major parts. First, the RFID reader itself and second, one or more transponders. The main difference between this system and other current systems is the channel access method in the uplink (transponder to reader communication) layer, in this case based on CDMA; this fact is illustrated in Figure 3 showing each transponder (Transponder 1 to Transponder n) with a unique spreading code (Code 1 to Code n).
The basic working principle is also indicted in Figure 3, showing the RFID reader transmitting a sinusoidal wave over its transmit antenna TX, thus allowing the various transponders in the field to modulate and reflect (principle of backscatter) this incident wave back to the RFID reader. Therefore, the total backscattered signal consists of the additive superposition of n (if multipath is negligible) backscattered transponder signals with each transponder using its own unique spreading code. Receiving this superimposed signal over RX, the reader is, generally, able to separate the various transponder signals from each other (process of despreading) in order to restore the transponders' data.
Figure 3 and Figure 5, respectively, show the concept and the architecture of the realized RFID reader. The following paragraphs will refer to these figures. Fig. 6 shows the setup of the system for directly measuring the backscattered baseband signals.

4. Implementation

Within this section, the implementation of the CDMA-based RFID system is described. By referring to Figure 4 and 5, Subsection 4.1 describes the overall *TX path*, involving the PLL-based RF synthesizer, a power amplifier (PA) and the TX antenna, whereas Subsection 4.3 reveals the fundamentals of the *RX path*, consisting of RX antenna, low-noise amplifier (LNA), a demodulator module, a baseband processing unit, a baseband sampling module (ADC module) and a subsequent DSP module for evaluating the incoming data. However, the basics of the *transponder* are depicted in Subsection 4.2.

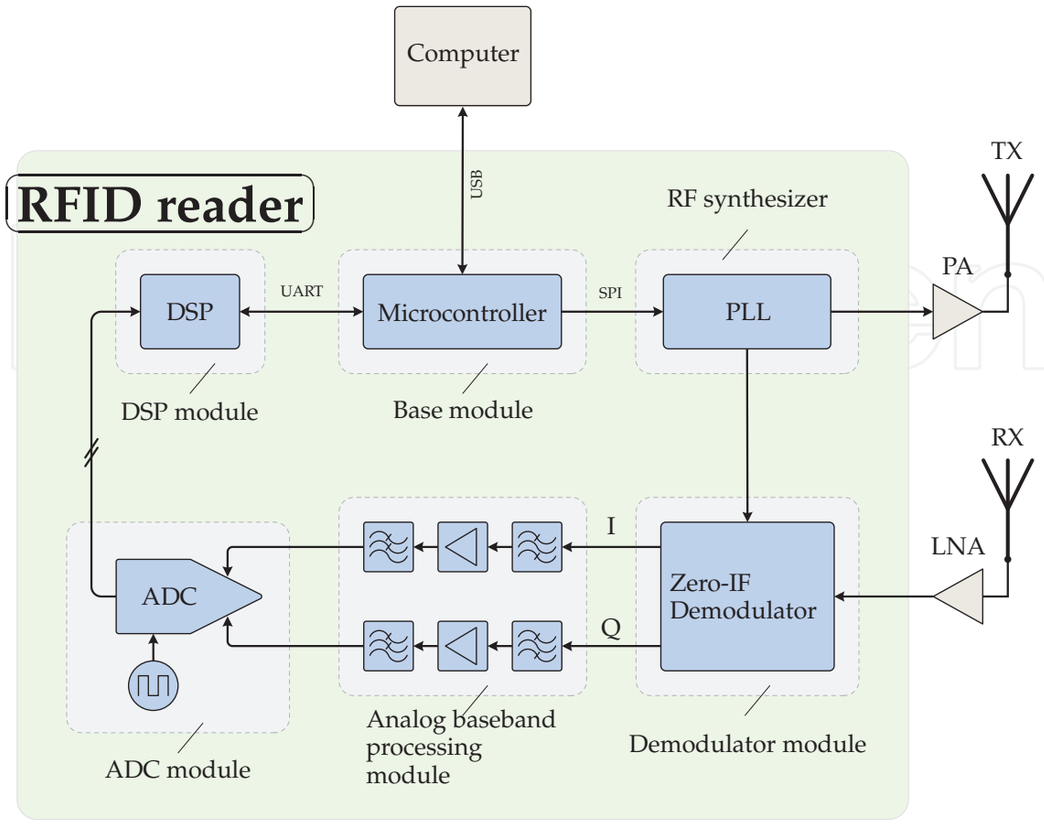

Fig. 4. Basic concept of RFID reader; depicted in bistatic antenna configuration

4.1 TX system path

The proposed semi-passive UHF transponder works in accordance with the principle of backscattering. The incident wave to be backscattered is generated by the *Transmitting System*. Considering the RFID uplink channel (tag to reader), the introduced *Transmitting System* (see Figure 3 and Figure 5) consists of a PLL-based RF synthesizer (Figure 3 and Figure 5) , generating a sine wave (here with $f_{\text{carrier}} = 866.5$ MHz, maximum output power $P_{out} = 1$ dBm at 50 Ω), an upstream power amplifier (PA, Gain $G_{PA} = 20$ dB, 1 dB compression point = 24 dBm), and a linear polarized 50 Ω antenna (TX, Gain $G_{TX} \approx 7$ dBi). The purpose of the transmitter is to generate an RF wave to be reflected (backscattered) by the UHF transponder whereby the reflected wave is received by the *Receiving System* further discussed in Subsection 4.3.

It has to be mentioned that the RF synthesizer not only generates a sine wave for the transmitting part, but also for the receiving part of the system. Indeed, it is used as local oscillator (LO) source for the downmixing part of the receiver. However, both synthesized RF waves inherit the same frequency as they are both created by the same PLL; the waves only differ in π in phase.

4.2 Transponder

The major tasks of the semi-passive UHF transponders are:

- Generate spreading code
- Create spreaded data

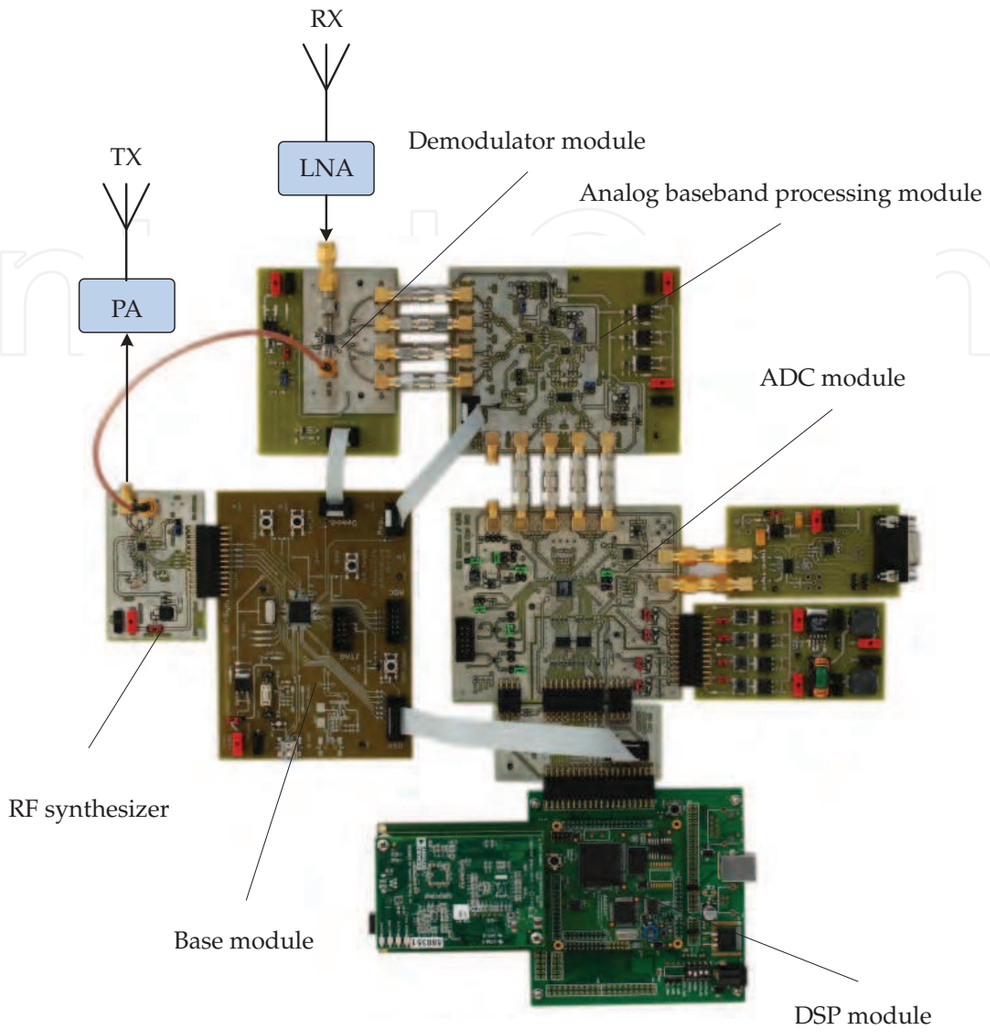

Fig. 5. Architecture of CDMA-based RFID reader

- Modulate and reflect incoming RF signal at $f_{\text{carrier}} = 866.5$ MHz (principle of backscatter)

Figure 7 shows the basic principle of an RFID transponder. An incident RF wave is reflected by the transponder. The phase and amplitude of the reflected wave is affected by three major issues: The first two issues includee structural mode and antenna mode scattering (Hansen, 1989; Penttila et al., 2006), the third issue is the multipath propagation. Multipath effects are a non-changeable fact, so they can be neglected at this point. The structural mode scattering of an antenna is dependent on the structure of the antenna itself (material, antenna geometry, etc.) and cannot be changed - therefore, the structural mode may not be used for a normal data transmission. The antenna mode scattering, on the other hand, describes the receiving and emitting effects of an antenna, which usually depend on the impedances used; particularly the impedance of the antenna Z_{ant} itself and the corresponding load impedance Z_{load} of the following transponder system. Assuming that Z_{load} can adopt two values being Z_1 and Z_2. According to Figure 7 the antenna mode scattering may be changed by altering the load impedance Z_{load} of the transponder's antenna according to the data the transponder

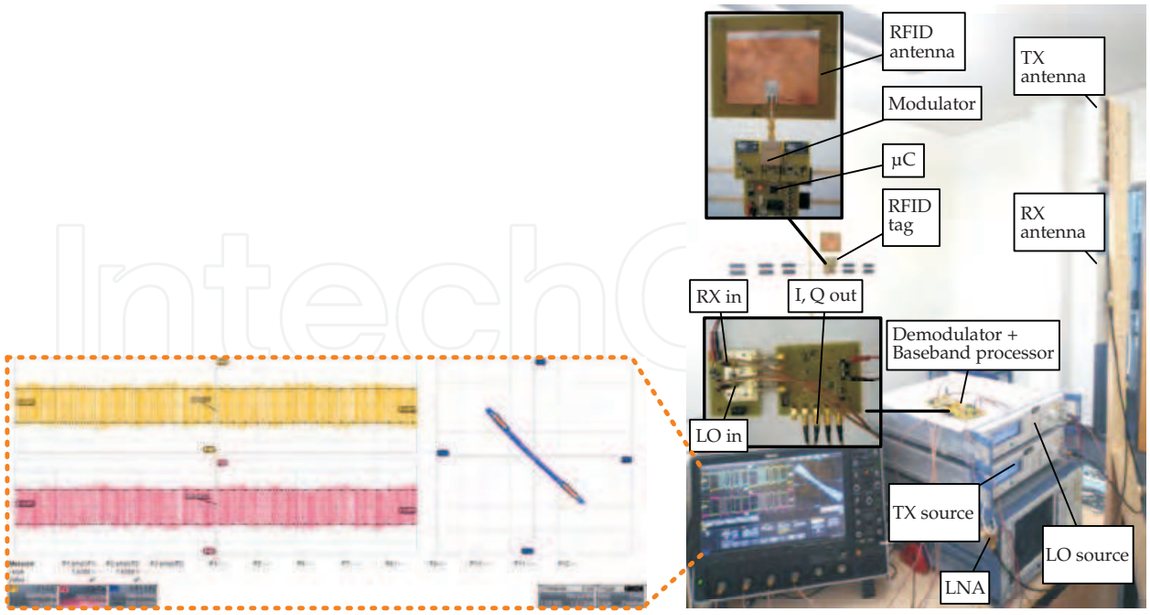

Fig. 6. Setup of CDMA-based UHF-RFID system with a magnification of the oscilloscope's screen

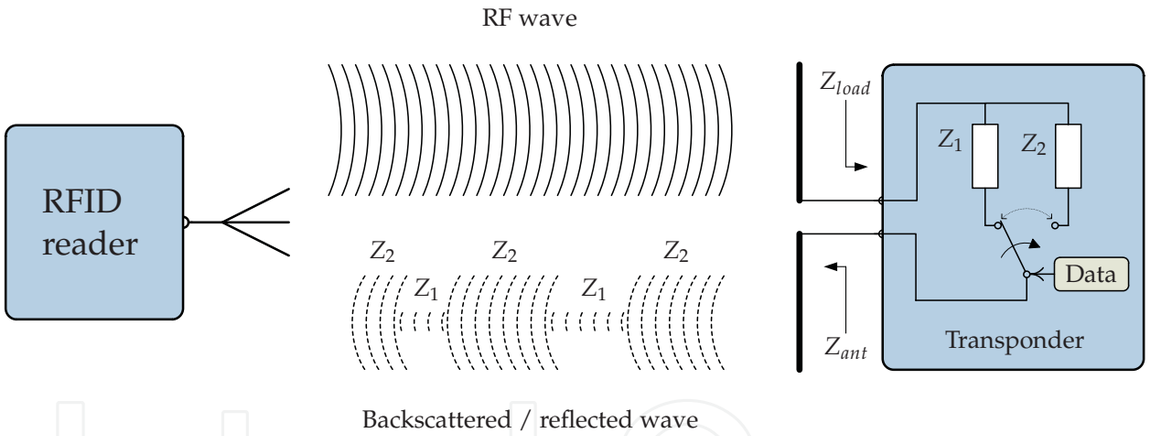

Fig. 7. Basic function of RFID transponder

wants to send. Binary data may be send by altering Z_{load} between Z_1 and Z_2, thus changing the reflection coefficient between Z_{ant} and Z_{load}, which in turn leads to an alteration of the reflection of the RF wave in phase and/or amplitude. Again, this only affects the antenna mode scattering. However, the total resulting backscattered signal is the superposition of the multipath signal, the structural mode scattering and antenna mode scattering effects. Measurements at the end of this paper will show this effects.

Figure 8 shows the basic concept of the CDMA-based semi-passive transponder. A central microcontroller generates the binary output data stream (i.e., the already coded and spreaded user data) to drive the fast RF switch 'S', that alters between two impedance states Z_1 and Z_2; according to the binary state of the output data stream, a logical '1' triggers Z_2, a logical '0' triggers Z_1 to be the corresponding load impedance. Therefore, the data stream directly affects the reflection coefficient. The performance of the uplink (tag to reader radio channel) depends

very much on the modulation efficiency η_{mod} of the backscatter modulator (Fuschini et al., 2008; Karthaus & Fischer, 2003; Nikitin & Rao, 2008), which basic calculation is subject of the following paragraph.

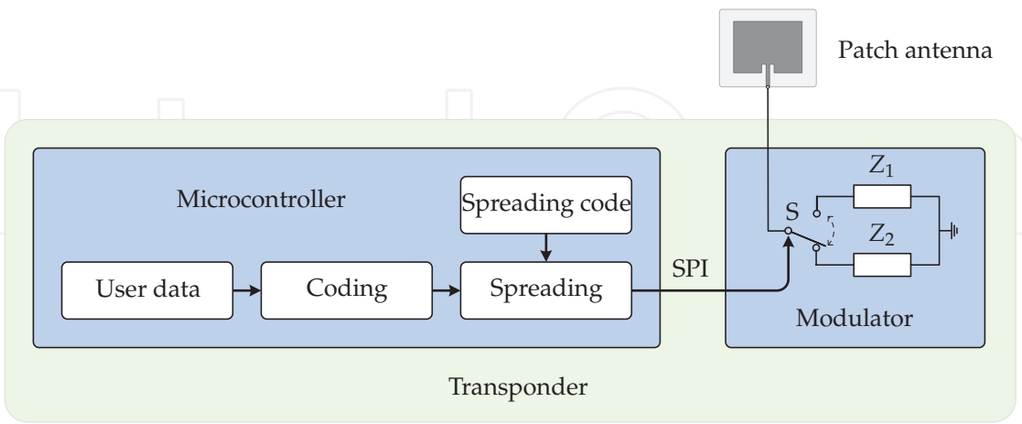

Fig. 8. Concept of CDMA-based semi-passive UHF RFID transponder

4.2.1 Determining load Impedances

Assuming an antenna with complex antenna impedance

$$Z_{ant} = R_a + j\,X_a \tag{4}$$

with $R_a = R_r + R_l$ as the sum of radiation resistance R_r and real antenna losses R_l, and X_a as the imaginary part of the antenna impedance. The complex reflection coefficients $\Gamma_{1,2}$ between the antenna impedance and the load impedances $Z_{1,2}$ can be described as

$$\Gamma_{1,2} = Z_{1,2} - Z^*_{ant}$$

with U_0 as the antenna's open circuit voltage and a being the wave from the antenna impedance to the load impedance (see Rembold (2009) for details).
Maximum modulation efficiency η_{mod} is achieved when the difference of the complex reflections coefficients Γ_1 and Γ_2 is maximum. Supposing two vectors (Γ_1 and Γ_2) in a complex coordinate system, the maximum difference between both vectors is achieved at the point when the phase φ_Γ differs with π under the assumption that the maximum absolute value of any Γ is limited to 1. That determines the complex reflection coefficients $\Gamma_{1,2}$ to

$$\Gamma_1 = e^{j\varphi_{\Gamma,1}} \tag{9}$$

$$\Gamma_2 = e^{j\varphi_{\Gamma,1}+j\pi} \tag{10}$$

Setting $\varphi_{\Gamma,1}$ to 0 sets $\Gamma_{1,2}$ to ± 1. According to Equation (5) this will define the load impedances to

$$Z_{1,2} = \frac{Z^*_{ant} + \Gamma_{1,2}\, Z_{ant}}{1 - \Gamma_{1,2}} \tag{11}$$

$$\rightarrow Z_1 = \frac{Z^*_{ant} + Z_{ant}}{0} = \pm\infty \tag{12}$$

$$\rightarrow Z_2 = \frac{Z^*_{ant} - Z_{ant}}{2} = \frac{-2jX_a}{2} = -jX_a \tag{13}$$

The antenna designed for the RFID transponders is a 50 Ω patch antenna (Figure 10). Therefore the imaginary part (within the specified frequency range) $X_a \approx 0$. This determines $Z_2 = -jX_a \approx 0$. A load impedance of $Z_1 = \infty$ corresponds to an open circuit wheres $Z_2 = 0$ corresponds to a short circuit. Choosing open and short circuit states as desired load impedances, the maximum achievable modulation efficiency is, according to Equation (7), determined to be

$$\eta_{mod} = \frac{2}{\pi^2}\,|+1+1|^2 = \frac{8}{\pi^2} \approx 81\% \tag{14}$$

In order to have the maximum modulation efficiency for the CDMA-based RFID system, the load impedances of the realized semi-passive transponders are set to open and short circuit. By choosing these values as load impedances, one has to keep in mind, that this is only advisable for semi-passive UHF RFID transponders. If passive transponders are designed, one has to consider the power consumption into its calculations. Therefore, open and short circuit values are not suitable, as the backscattered power is, in fact, too high, as the transponder needs a large portion of the incoming power for supplying itself (Dobkin, 2008).

4.2.2 Transponder basics

Figure 9 illustrates the concept of the transponder and Figure 10 shows one of the realized transponders to achieve the previously mentioned tasks. The microcontroller (µC) is powered by a power supply and may be user-controlled using USB or pushbuttons. The µC generates the unique spreading code and subsequently, the spreaded outgoing data. The data are forwarded to the SPI interface to drive the modulator of the transponder with different input voltages to adjust different load impedances respectively reflection coefficients of the modulator. The block diagram of the modulator (Figure 8) shows the principle of the proposed simple backscatter modulator. An example on how to design load modulators can be found in Pardo et al. (2007). However, the incoming spreaded data stream is low-pass filtered to limit

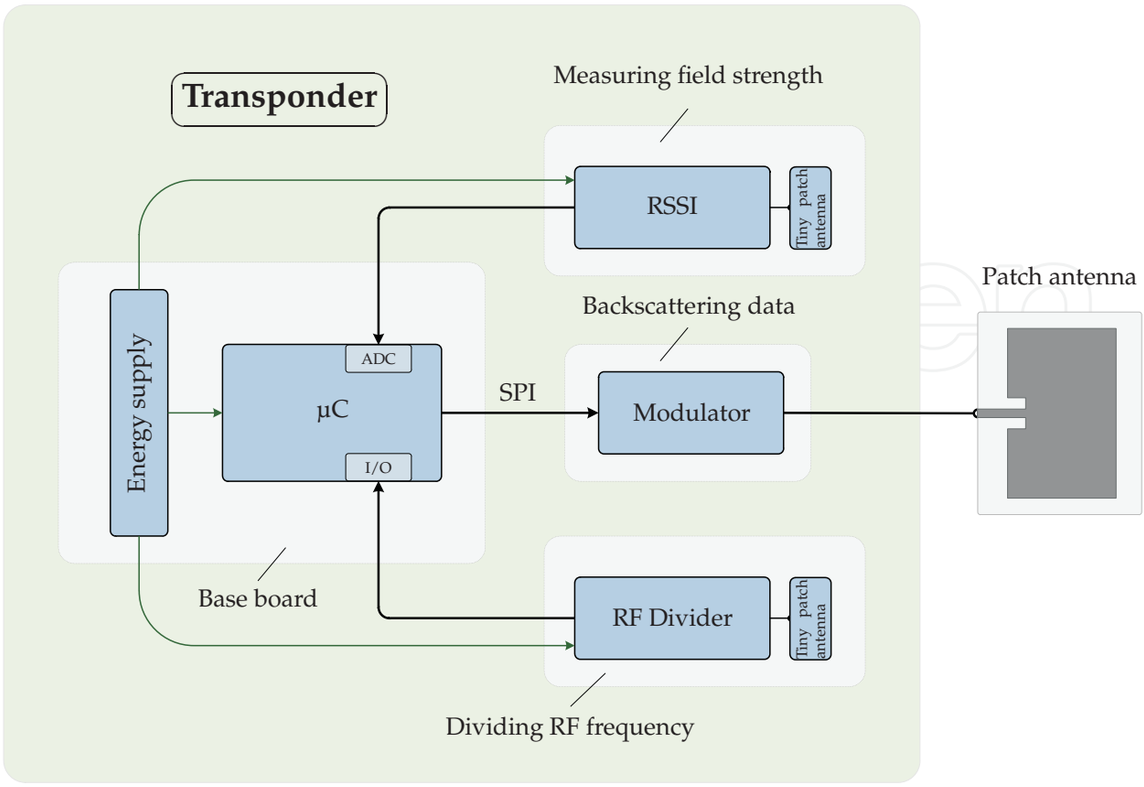

Fig. 9. Block diagram of semi-passive UHF RFID transponder with limited downlink capabilities

the outgoing bandwidth. As the modulator should be as simple as possible, an RF switch 'S' forms the interface between the logic data and the backscattered HF wave. The inputs of the switch are driven by the spreaded data stream with two voltage levels (0 and 2.75 V) given by a buffer driver. One connection of the switch is linked to the patch antenna's microstrip line (50 Ω); the ground connection is linked to the patch antennas ground plane. By triggering the switch's input with the spreaded data to be sent, either Z_1 or Z_2 is connected to the antenna. This modification changes in turn the reflection of an incident electromagnetic wave. The difference of phase and amplitude of the reflection is a direct indicator for the efficiency of a backscattering modulator. As mentioned above the modulators load impedances are set to open and short circuit to achieve maximum modulation efficiency. An exemplary spectral extract of the backscattered output of the transponder, measured at the receiving antenna, is given in Figure 17. On closer inspection, one can see the spreaded data (chip rate is 1.5 Mcps) around the carrier frequency (866.5 MHz). As these data signal levels ($P \approx -90$ dBm $\pm$ 10 dB) are not very high, an accurate implementation of the receiving system becomes necessary.
For a limited downlink (reader to tag) capability the transponders are equipped with a module for measuring the field strength (RSSI) and a module for measuring the frequency (RF Divider) of the incident RF wave emitted by the reader. The *RF Divider* is currently used to indicate the transponder to send its data as soon as a carrier between 865 MHz and 868 MHz is detected. The RSSI module is used for statistical measurements. Anyway, both modules are not part of this work.

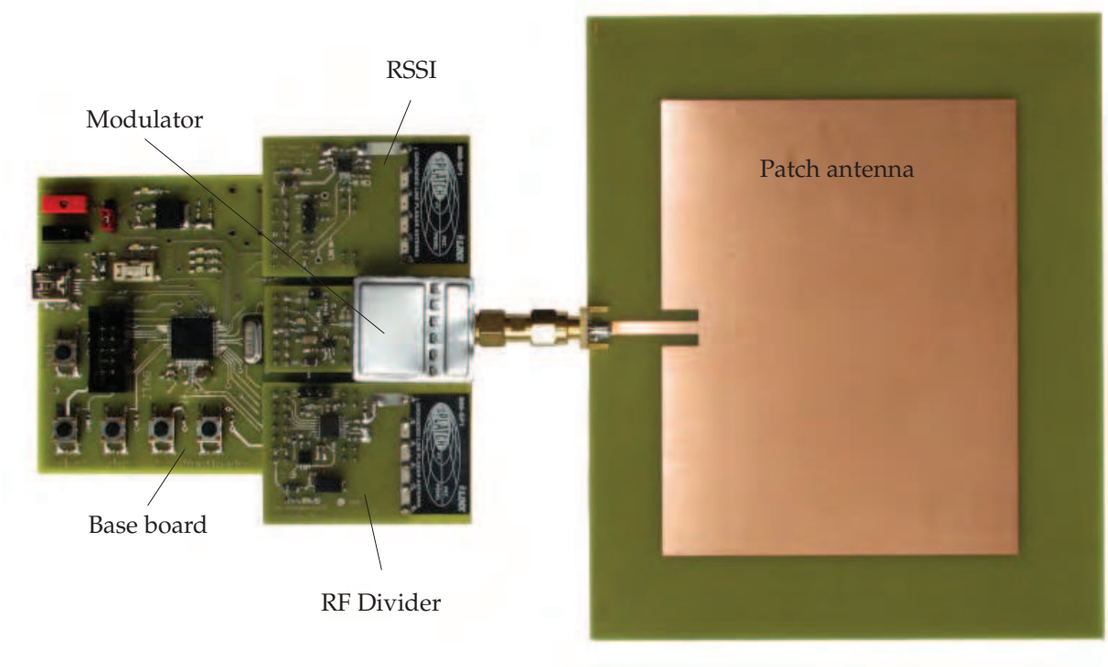

Fig. 10. Prototype of semi-passive UHF RFID transponder

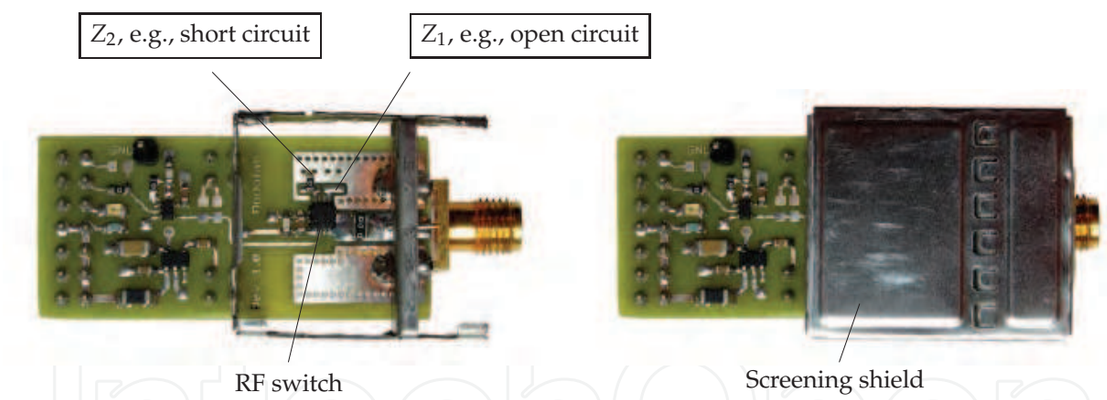

Fig. 11. Backscatter modulator

4.2.3 Modulator

The transponder's modulator is one of the key components of the system. Usually, it effects the energy supply (only for passive working transponders) and the modulation efficiency (for passive and semi-passive working transponders) of transponders. Therefore, it has a direct effect for the maximum achievable range of such a system. The principle of the modulator has been already discussed above, so that this paragraph focuses primarily on the realization. Figure 11 shows the modulator, with and without RF shielding. The left part of the modulator is connected to the transponder's base board, the right SMA plug to the patch antenna as shown in Figure 10. The part within the RF shielding is responsible for the backscattering effects. A part of the incident RF wave is fed into the modulator. The part depends on the antenna (structural and antenna mode) and the reflection coefficient between antenna

impedance Z_{ant} and the load impedance Z_{load} of the connected modulator. This part is fed into the RF switch and the load impedance (either Z_1 or Z_2), which corresponds to the current state of the switch. The state of the switch is defined by a buffered microcontroller output. which itself shows the current voltage of the binary data stream to be sent. In the case of Z_1 (open circuit state), the incident wave is entirely reflected with no phase shift. State Z_2 (short circuit) also corresponds to a total reflection, but with a phase shift of 180°.
Measuring the load impedances of the modulator show a very good accordance with the theoretical results. Figure 12 shows the reflection coefficients within a Smith chart. As one can see the phase difference is not exactly π. Z_2 (short circuit) has nearly short circuit properties; Z_2 (open circuit) has nearly open circuit properties. The frequency range of the measurement was between 852 MHz and 882 MHz.

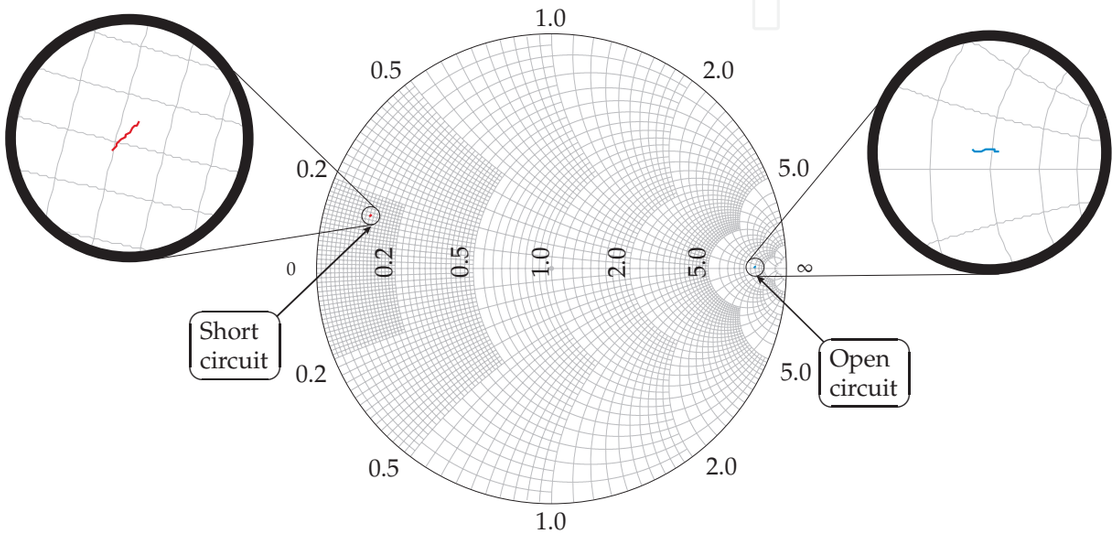

Fig. 12. Smith chart of modulator

4.2.4 Gold codes

The choice of an appropriate set of spreading codes is a key issue when designing CDMA systems. Gold codes seem to be one of the best codes to be used in UHF RFID systems. Mutti & Floerkemeier (2008), for instance, state that Gold codes outperform Kasami codes. Moreover, one Gold code family contains a large number of unique codes, which provides a high probability of finding a well-suited set of codes for a system to be designed.
Gold codes, first introduced by Robert Gold (Gold, 1967b), are commonly used in spread spectrum systems, such as WLAN and UMTS as well as in GPS (C/A code). The generation of Gold codes is quite simple as only two linear feedback shift registers (LFSR) are necessary to create one set of codes. Other advantages of Gold code are:

- Good balance between auto- and cross-correlation
- Flexibility in code length
- No user synchronization necessary, i.e. the transponders need not to be synchronized among each other

Because of above mentioned advantages, the proposed CDMA-based system uses Gold sequences.

However, Gold codes have a length of $2^m - 1$ with m being the order of each linear feedback shift register. For reasons of flexibility a Gold code generator has been implemented on the transponder's 32 bit µC. The choice fell upon a Gold code length of 127 ($m = 7$). The characteristic polynomial is 137_{dec} for the first LFSR and 143_{dec} for the second one. The initial value for the first LFSR is 85_{dec}. By choosing two Gold codes (Code 1 and Code 2) the second LFSR is initialized with 127_{dec} for the first and with 111_{dec} for the second code. Then, a small adjustment was made to the generated Gold codes to be more compatible to the µC. A succeeding binary '0' is added to each code to move it to a length of 128 bit. To show the effect of this '0', the auto-correlation function (ACF) and cross-correlation function (CCF) have been evaluated for both Codes. Figure 13 shows the ACF Φ_{cc} of the original 127 bit Gold codes. Figure 14 illustrates the ACF $\Phi_{cc}(\tau)$ of the adjusted (127+1 bit) Gold codes. The results are slightly higher values beyond the peak value at $\tau = 0$. As not only the auto-correlation counts, the corresponding cross-correlation $\Phi_{1_2}(\tau)$ between the two codes are presented in Figure 15. As expected the values of the adjusted codes are slightly higher compared to the original ones, but without loosing the typical noise-like character. This means, that the effect of the added '0' is negligible for further considerations. However, final system implementations have to consider that fact.

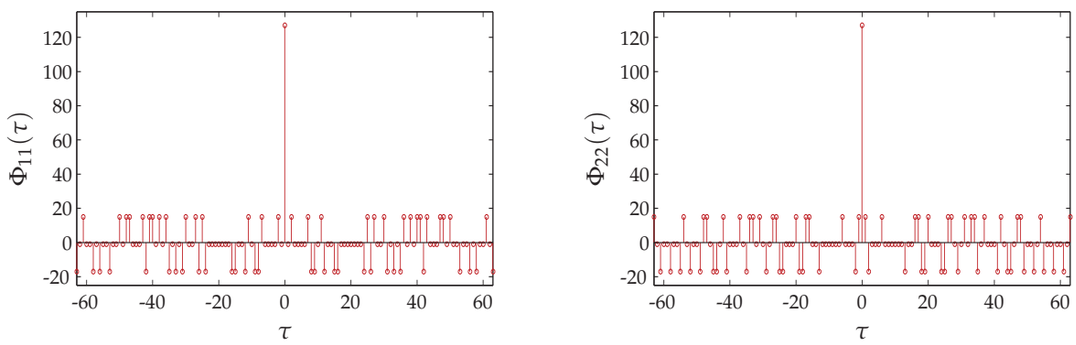

(a) ACF of Code 1 (b) ACF of Code 2

Fig. 13. ACF of original Gold codes

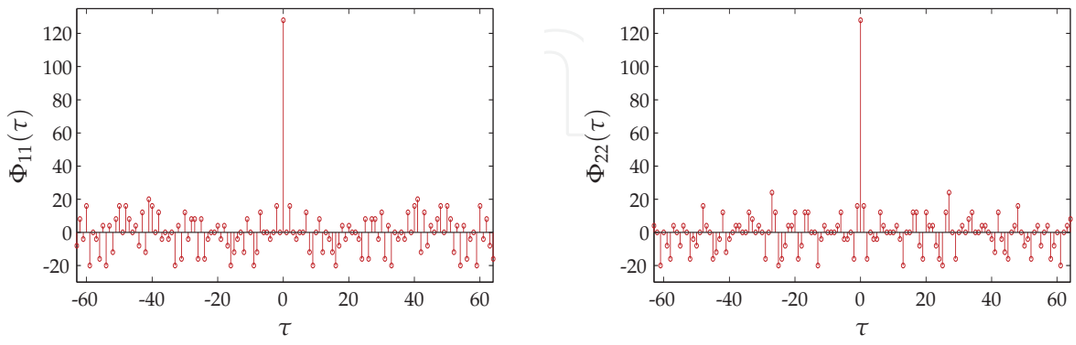

(a) ACF of Code 1 (b) ACF of Code 2

Fig. 14. ACF of adjusted Gold codes

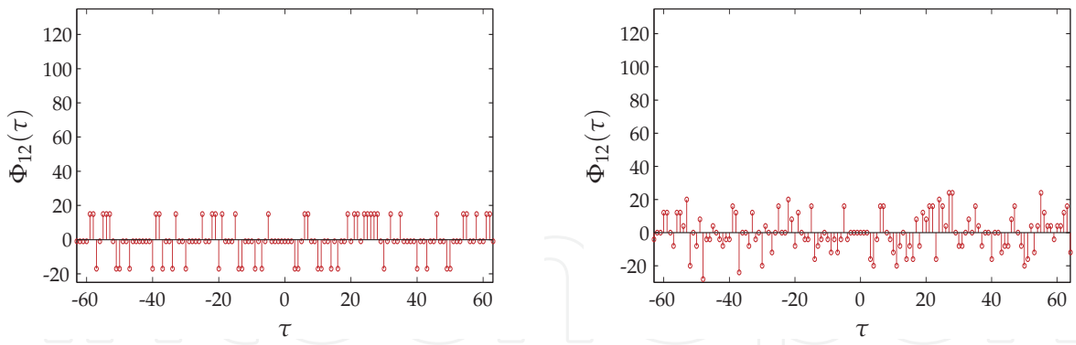

(a) CCF of original Code 1 and Code 2 (b) CCF of adjusted Code 1 and Code 2

Fig. 15. CCF of both, original and adjusted Gold codes

4.3 RX system path

The major tasks of the *Receiving system* are:

- Receive incoming signals from several transponders, i.e., downmixing, analog baseband processing and A/D conversion
- Find separate data streams (transponders) by despreading, demodulating and decoding the signals

The *Receiving system* mainly consists of a hardware part that is needed to mix down the backscattered RF signal, centered at $f_c = 866.5$ MHz, into baseband, despread, demodulate, and decode the baseband signal in order to determine the transponders' data. Figure 16 presents the structure of this receiving part of the RFID reader. The incoming RF signal is caught by a receiving antenna (RX) and amplified by a following low noise amplifier (LNA). A subsequent Zero-IF IQ-Demodulator mixes down the RF signal directly to baseband. The output of the demodulator consists of differential I- and Q-signals, which are band-pass filtered, twice amplified and active low-pass filtered. It has to mentioned that the IQ signals are completely handled differentially throughout the amplifier and filter stages to keep the signal-to-noise ratio (SNR) at a high level. The succeeding Analog-to-Digital conversion (ADC) module samples both, the I- and Q-signal, simultaneously. The A/D converted signals are fed into a digital signal processor (DSP) block with a data rate of 450 Mbps (Sampling of 2 channels with each channel having a resolution of 15 bit (14 data + 1 status bit) including a sampling rate of 15 Msps). The DSP module despreads, demodulates and decodes this data stream. The results are the user data of each recognized transponder.
The following paragraphs focus on the details of the receiving system.

4.3.1 Demodulator

The incoming low-noise amplified signal is fed into the demodulator. The demodulator uses the second RF synthesizer signal (the first is used as RF signal source for the transmit path, see above) as local oscillator (LO) source, to mix down the RF signal directly into baseband (Zero-IF). The demodulator is based on the LT5575 chip (Linear Technology, 2010a) and is 50 Ω-matched between 865 MHz and 868 MHz. The output of the demodulator is differential with 2 I- and 2 Q-signals, respectively.

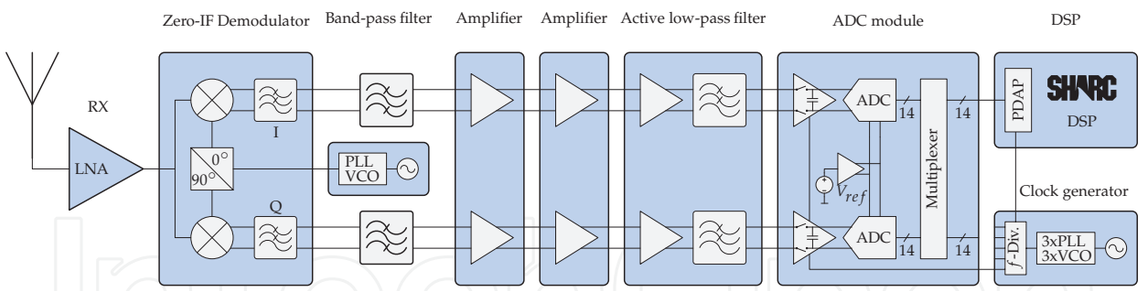

Fig. 16. Architecture of receiving system

4.3.2 Band-pass filter

The differential working band-pass filter, which succeeds the demodulator, is used to suppress the DC-part of the baseband signal, i.e. mainly the non-information carrying down-mixed carrier signal, and high-frequency disturbing signals (from the internal mixer of the demodulator). Therefore the passband is set between 16 kHz and 20 MHz.

4.3.3 Amplifier stage

The following amplifier stage is build upon two differential amplifiers (LTC6421-20 (Linear Technology, 2010d) and LTC6420-20 (Linear Technology, 2010c)), each with a differential voltage gain of 10 V/V.

4.3.4 Active anti-aliasing filter

The last analog signal processing stage is an active anti-aliasing filter for the succeeding ADC module. The cut-off frequency of the 4th order low-pass filter (Chebyshev characteristic) is currently set to 2.5 MHz. This stage is based on an LT6604-2.5 (Linear Technology, 2010b).

4.3.5 A/D conversion

One very important part of the receiving system is a well-designed A/D conversion stage for the baseband signal. The subjective of the ADC module is a time synchron sampling of the differential I- and Q-signals. The module is based on a dual A/D converter of type AD9248 from Analog Devices (2010a). Two channels may be sampled synchronously with a resolution of 14 bit per channel. Maximum sampling rate is 40 Msps. As the fast parallel input of the succeeding DSP module has only 20 bit the internal multiplexer of the A/D converter is used to transmit the I- and Q-data after each other. Therefore one status bit is used to indicate the current transmitted channel data. Here, the A/D converter is driven with 15 Msps per channel, which corresponds to an overall sampling clock rate of 30 MHz. The 14 bit per channel plus the status bit and the sampling rate, generate in total a data rate of 450 Mbps to be handled by the subsequent DSP module.

4.3.6 DSP module

The purpose of the DSP is the handling of all calculations, necessary to evaluate the transponders' user data. Therefore, the following stages are necessary:

- Data acquisition (from ADC module)
- Despreading of baseband signals
- Demodulation of despreaded signals
- Decoding of demodulated data

The following paragraphs give a short introduction to these topics. The data acquisition phase has to be accomplished only once, against what the following stages have to be passed through by every transponder respectively spreading code available.

4.3.6.1 Data acquisition

As the amount of data to handle is quit large (450 Mbps) the data streams are not handled in real time. However, through the usage of this DSP (ADSP-21469 from Analog Devices (2010b)) the processing speed is quite high. The A/D converted data signals are acquired through the DSP's PDAP (Parallel Data Aquisition Port) interface. From there, they are transfered to an internal 8x32 bit buffer. Finally, the data are passed via DMA access to an internal memory. As of limited memory capabilities the data is transferred block-wise to the external memory. As the sampled values are stored as 32 bit values (DWORD), the amount of data for one shot (duration is $T_{shot} \approx 188$ µs) is 90112 samples per channel, so in total 720896 bytes or 704 kbytes.

4.3.6.2 Despreading

The process of despreading is the most calculation intensive operation the DSP has to handle. As this phase needs more time than the data acquisition process the system is, up-to-date not able to work real-time. Parallel processing would be a good solution. The DSP itself has a clock rate of 450 MHz.
Despreading data from the baseband signal has to be done for I- and Q-channel separately. The despreading operation is realized using the cross-correlation between I and Q signals and the origin codes used by every transponder in the field. If $s[k]$ is the I or Q signal and $c[k]$ one of the corresponding codes of one of the transponders, the cross-correlation $\Phi_{s,c}(\tau)$ between these signals is done by multiplying every time instance signal s with code c. Equation (15) shows the corresponding relationship between $c[k]$ and $s[k]$, whereas ★ matches the convolution function:

$$[s \bigstar c][\tau] = \Phi_{s,c}(\tau) = \sum_{t=-\infty}^{+\infty} s^*[t] \cdot c[\tau + t] \tag{15}$$

A code length of 128 chips corresponds to 1280 samples ($R_{chip} = 1.5$ Msps and $R_{sample} = 15$ Msps) and 90112 samples per channel for I and Q. This results into 230,686,720 multiplications and 180,224 additions.
One goal was to reduce this high amount of operations. This is realized through estimation of the time moments the chips appear within the IQ signals. This estimation method works as follows. The IQ baseband signal is sampled and correlated among the first $2 \cdot 1280 = 2560$ samples. This results in 6,553,600 multiplications and 5120 additions. The first maximum, corresponding to the first peak indicates the initial index i_0 to start the despreading process. The following peaks are estimated by jumping from i_0, 1280 samples ahead. As certain incertitudes (oscillators, etc.) will lead to synchronization errors, the correlation is not only made at sample index $i_0 + n \cdot 1280$, but at 5 samples before and after the estimated time index. That means, the second peak is determined by executing the cross-correlation $\Phi_{i,1}(\tau)$ as given in Equation (16).

$$\Phi_{i,1}(\tau) = \sum_{t=i_0+1280-5}^{i_0+1280+5} s^*[t] \cdot c[\tau + t] \tag{16}$$

The result is 11 correlations per peak and a new synchronization index, as the new peak indicates the next starting point for the succeeding peak estimation. With 70 data peaks within one shot and 1 within the initial guess, the total number of correlations per channel

is $2560 + 69 \cdot 11 = 3319$. This leads to 8,496,640 multiplications and 6,638 additions in total for both channels. This is only 3.6% of the full correlation.

4.3.6.3 Demodulation

The process of demodulation inherits the merge of the I and Q signals. According to their signal quality, estimated through the maximum correlation values, the signals are weighted and superimposed. This process of demodulation is beyond this paper's scope and not further described.

4.3.6.4 Decoding user data

The demodulated signal stream is Manchester coded (Loeffler et al., 2010) and needs to be decoded accordingly. The resulting data stream corresponds to the transponder's respectively the user data.

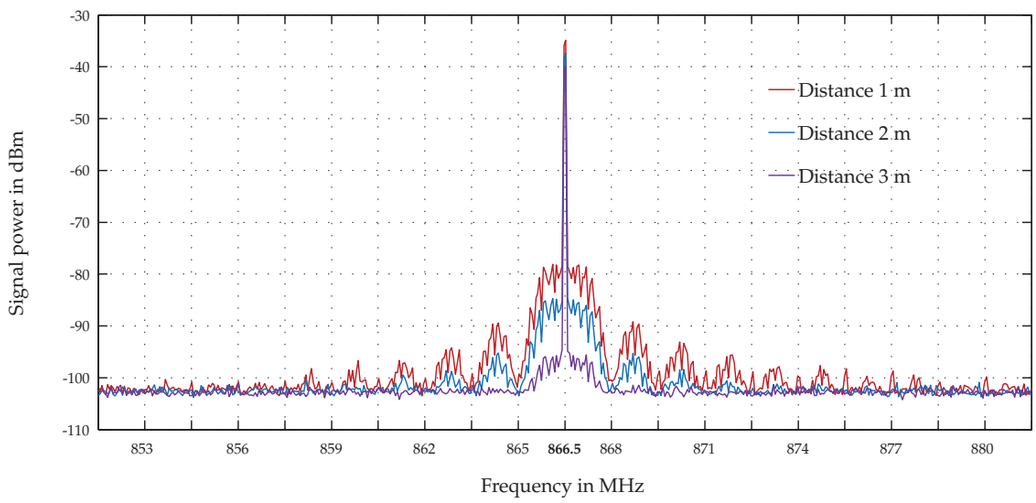

Fig. 17. Spectrum of backscattered signal from transponder

5. Measurements

This section presents measurements of various parts of the system, including transponder, analog baseband processing and DSP.

5.1 Transponder measurements

Figure 17 shows the spectrum of the backscattered transponder signals. For this measurement an RF signal ($P_{TX} = 10$ dBm, $f_{\text{carrier}} = 866.5$ MHz) is fed into the linear polarized transmit antenna. One transponder is placed at a distance of 1, 2 and 3 m. The resulting reflected signal spectrum after the receiving antenna is shown in Figure 17. As expected, the backscattered signal parts drop with increasing distance from the reader's antennas.

The IQ constellation diagrams of the received RF signal are shown throughout Figure 18(a) to Figure 18(c). It can be shown that the backscattered signals show a mixture between ASK and PSK modulation. For instance, as in Figure 18(a), the mean of the data points (from the two states of the one transponder) is not the origin (0,0). This discrepancy is the effect of multipath and structural antenna mode scattering. Same applies for Figure 18(b) with 2

transponders, generating $2^2 = 4$ constellation points, and Figure 18(c) with 3 transponders, generating $2^3 = 8$ constellation points. The number of constellation points for n transponders is 2^n because all n transponders have 2 states sharing the same coherent RF signal from the reader.
However, as expected the transponders show a near exact BPSK modulation (as configured in Subsubsection 4.2.3), if the ASK part is neglected.

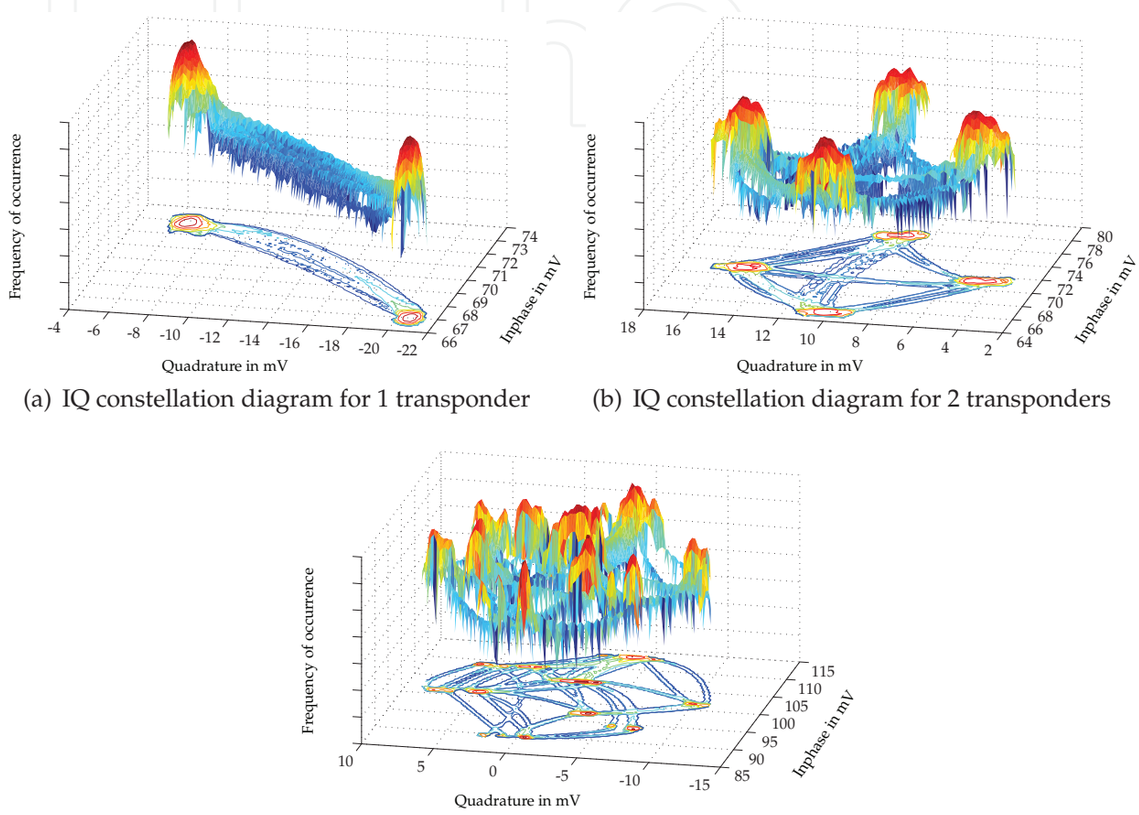

(a) IQ constellation diagram for 1 transponder

(b) IQ constellation diagram for 2 transponders

(c) IQ constellation diagram for 3 transponders

Fig. 18. Various IQ constellation diagrams for 1, 2 and 3 transponders in the field of the reader

5.2 RX measurements

Two measurements have been carried out to show the basic working principle of the analog baseband processing module. The goal of this module is the signal conditioning for the succeeding ADC module. Figure 19(a) shows the output of the demodulator, i.e. the I- and Q-signals. As mentioned above these signals are handled differentially (I_+, I_-, Q_+ and Q_-). To simplify matters the differential signals have been put together ($I = I_+ - I_-$ and $Q = Q_+ - Q_-$) . The signals are amplified and filtered with a resulting signal as shown in Figure 19(b). The signals were recorded with 2 transponders in the field. As in the IQ measurements before, 2 transponders generate $2^2 = 4$ different signal levels (evaluated from Figure 19(b)) leading to a quasi QPSK-like signal with an elliptic distribution of the absolute

values:

$$\begin{aligned} 0.1\ \mathrm{V} + j0.2\ \mathrm{V} &\equiv 0.23\ e^{+j49.4^\circ} \equiv 0.23\ e^{j0^\circ} \\ 0.3\ \mathrm{V} - j0.4\ \mathrm{V} &\equiv 0.55\ e^{-j50.5^\circ} \equiv 0.55\ e^{j260.1^\circ} \\ -0.2\ \mathrm{V} - j0.2\ \mathrm{V} &\equiv 0.27\ e^{-j123.7^\circ} \equiv 0.27\ e^{j186.9^\circ} \\ -0.4\ \mathrm{V} + j0.5\ \mathrm{V} &\equiv 0.59\ e^{-j233.6^\circ} \equiv 0.59\ e^{j77.0^\circ} \end{aligned} \tag{17}$$

Although the phase relations between the different states is about 90° in this measurement, usually the phase is randomly distributed, being dependent on the geometric formation between transponder and reader antennas. This snapshot was taken because of easy visibility.

5.3 DSP measurements

The DSP module comes with some debugging functionalities. One of these functionalities is able to provide the DSP values, from its internal or external memories, via USB to a host PC. Figure 20 shows the results of a full cross-correlation. For simplicity the CCFs have been normalized to one. The values show the maximum number of samples (90112) and the peaks, with each peak describing a bit. The value of the bit may be positive (+1) or negative (−1). The difference between the peaks and the noise floor is an indicator for the quality of the communication link.

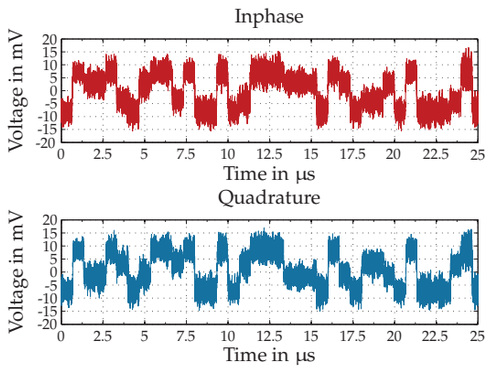

(a) IQ signal after demodulator / 2 Transponders

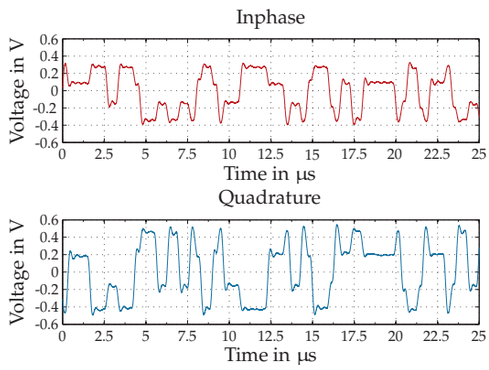

(b) IQ signal after baseband processing / 2 Transponders

Fig. 19. IQ signals after demodulator (right) and after baseband processing (left)

6. Results

According to the measurements the proposed system worked as expected. It was proved that the UHF RFID system for broadcasting information data using a CDMA method worked out very good. During the experiments there was a maximum distance to the antennas being around 15 m. The transmitted RF-power at 866.5 MHz was 20 dBm. The introduced transponders are semi-passive, which means that the communication link is still passive, whereas the data generation (on the transponder's side) is active, driven by 3.3 V power supplies.

Smaller problems arose, when various transponder had a different path length to the antennas. In that case one transponder (the nearest) dominated the second transponder (more far away) which often occurred to a non-detection of transponder two. This problem is known

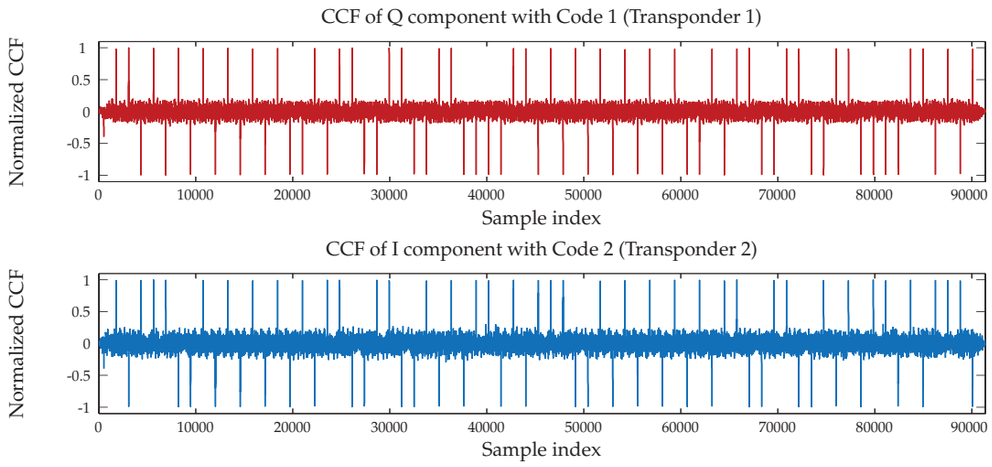

Fig. 20. Cross-correlation of signals with origin spreading codes - Process of despreading / 2 Transponders

in CDMA systems and is referred to as near-far problem (Andrews, 2005). One possibility to reduce the near-far effect is the usage of Huffman sequences (Liu & Guo, 2008). But this approach asks for more than 2 states of the load impedance of the transponder's modulator. Nevertheless, carried out indoor experiments showed that the near-far effect of the proposed system is, in fact, very low.
Also, theoretical work, which states an advantage (this statement is only valid for certain cases) of CDMA-based RFID systems compared to state-of-the-art RFID systems based on TDMA methods, complies with the measured results of the proposed CDMA-based UHF RFID system.

7. Conclusion

This article presented an implementation of a CDMA-based RFID system working in the UHF region. At the beginning the article gave a short introduction to anti-collision methods used in RFID technology. Subsequently, a performance comparison was made to show the effect of using CDMA in RFID. It could be stated, that CDMA does outperform traditional TDMA methods, but only in particular fields of applications. The implemented RFID system itself is build upon a *Transmitting system* providing a continuous electromagnetic wave. This emitted RF carrier is backscattered through one or more designed UHF tags. Each of these semi-passive operating transponders generate a unique spreading sequence. The proposed spreading sequences are Gold codes providing a good orthogonality. A simple modulator on the transponder generates the desired backscatter signal. The *Receiving system* captures this signal by down mixing the RF signal to baseband. Further analog signal processing and subsequent A/D conversion gives the DSP the chance to despread, demodulate and decode the desired transponder signals.
The significant advantage of such a structure compared to present systems lies in the ability to avoid particular TDMA-based anti-collision schemes. Certainly, this will lead to less time needed for *inventorizing* RFID tags, as this can be achieved within one time slot. However, the number of tags to be read this way, is somewhat limited (due to the usage of CDMA), whereas TDMA methods may recognize a huge amount of transponders, indeed, at the expense of time to identify. Finally, one can say, that the deployment of CDMA is useful in cases where the number of transponders has an upper limit or is fixed. For such cases the time for detection

may be minimized using appropriate spreading codes. Fields of application mainly include closed systems, e.g., found in industrial facilities.

8. Acknowledgment

I would like to thank Fabian Schuh, and in particular Ingo Altmann, without whom this publication would not have been possible. His ideas, work, and research on this topic made a big contribution to this chapter. Also, I would like to thank my colleagues for their very productive ideas and valuable discussions.
To my wife Sonja, my daughters Jenny and Jolina, and my son Tom, for having the patience with me, despite my long periods in the office which decrease the amount of time I can spend with them.

9. References

Abramson, N. (1970). THE ALOHA SYSTEM: another alternative for computer communications, *Proceedings of the November 17-19, 1970, fall joint computer conference*, AFIPS '70 (Fall), ACM, New York, NY, USA, pp. 281–285.
URL: *http://doi.acm.org/10.1145/1478462.1478502*

Aein, Joseph M. (1964). Multiple Access to a Hard-Limiting Communication-Satellite Repeater, *Space Electronics and Telemetry, IEEE Transactions on* 10(4): 159–167.
URL: *10.1109/TSET.1964.4337583*

Analog Devices (2010a). AD9248: Dual 14-Bit, 20/40/65 MSPS, 3 V Analog-to-Digital Converter.
URL: *http://www.analog.com/en/analog-to-digital-converters/ad-converters/ad9248/products/product.html*

Analog Devices (2010b). ADSP-21469: High Performance Fourth Generation DSP.
URL: *http://www.analog.com/en/embedded-processing-dsp/sharc/adsp-21469/processors/product.html*

Andrews, J. (2005). Interference cancellation for cellular systems: A contemporary overview, *IEEE Wireless Communications* 12(2): 19–29.

Bang, O., Kim, S. & Lee, H. (2009). Identification of RFID tags in dynamic framed slotted Aloha, *Advanced Communication Technology, 2009. ICACT 2009. 11th International Conference on*, Vol. 01, pp. 354 –357.

Bertsekas, D. & Gallager, R. (1992). *Data networks (2nd ed.)*, Prentice-Hall, Inc., Upper Saddle River, NJ, USA.

Choi, J. H., Lee, D. & Lee, H. (2007). Query tree-based reservation for efficient RFID tag anti-collision, *Communications Letters, IEEE* 11(1): 85 –87.

Cui, Y. & Zhao, Y. (2009). A modified Q-parameter anti-collision scheme for RFID systems, *Ultra Modern Telecommunications Workshops, 2009. ICUMT '09. International Conference on*, pp. 1 –4.

Dobkin, D. (2008). *The RF in RFID: passive UHF RFID in practice*, Newnes.

EPCglobal Inc. (2008). Class 1 Generation 2 UHF Air Interface Protocol Standard "Gen 2" v. 1.2.0.

Finkenzeller, K. (2003). *RFID handbook*, Wiley West Sussex, England.

Fuschini, F., Piersanti, C., Paolazzi, F. & Falciasecca, G. (2008). On the Efficiency of Load Modulation in RFID Systems Operating in Real Environment, *Antennas and Wireless Propagation Letters, IEEE* 7: 243 –246.

Gold, R. (1967a). Optimal binary sequences for spread spectrum multiplexing (corresp.), *Information Theory, IEEE Transactions on* 13(4): 619 – 621.

Gold, R. (1967b). Optimal binary sequences for spread spectrum multiplexing (Corresp.), *Information Theory, IEEE Transactions on* 13(4): 619 – 621.

Gopalan, S., Karystinos, G. & Pados, D. (2005). Capacity, throughput, and delay of slotted ALOHA DS-CDMA links with adaptive space-time auxiliary-vector receivers, *Wireless Communications, IEEE Transactions on* 4(1): 79 – 92.

Hansen, R. (1989). Relationships between antennas as scatterers and as radiators, *Proceedings of the IEEE* 77(5): 659 –662.

IPICO (2009). IPICO's IP-X RFID Air-interface Protocol.
URL: *http://www.ipico.com/*

Karthaus, U. & Fischer, M. (2003). Fully integrated passive uhf rfid transponder ic with 16, 7μw minimum rf input power, *IEEE* 38(10): 1602–1608.

Kleinrock, L. & Tobagi, F. (1975). Packet Switching in Radio Channels: Part I–Carrier Sense Multiple-Access Modes and Their Throughput-Delay Characteristics, *Communications, IEEE Transactions on* 23(12): 1400 – 1416.

Lee, D., Bang, O., Im, S. & Lee, H. (2008). Efficient dual bias Q-Algorithm and optimum weights for EPC Class 1 Generation 2 Protocol, *Wireless Conference, 2008. EW 2008. 14th European*, pp. 1 –5.

Linear Technology (2010a). LT5575 - 800MHz to 2.7GHz High Linearity Direct Conversion Quadrature Demodulator.
URL: *http://www.linear.com/pc/productDetail.jsp?navId=H0,C1,C1011,C1725,P36240*

Linear Technology (2010b). LT6604-2.5 - Dual Very Low Noise, Differential Ampli?er and 2.5MHz Lowpass Filter.
URL: *http://www.linear.com/pc/productDetail.jsp?navId=H0,C1,C1154,C1008,C1148,P85251*

Linear Technology (2010c). LTC6420-20 - Dual Matched 1.8GHz Differential Amplifiers/ADC Drivers.
URL: *http://www.linear.com/pc/productDetail.jsp?navId=H0,C1,C1154,C1009,C1126,P80614*

Linear Technology (2010d). LTC6421-20 - Dual Matched 1.3GHz Differential Amplifiers/ADC Drivers.
URL: *http://www.linear.com/pc/productDetail.jsp?navId=H0,C1,C1154,C1009,C1126,P80589*

Linnartz, J.-P. M. & Vvedenskaya, N. D. (2009). DS-CDMA Packet Network with Random Access.
URL: *http://www.wirelesscommunication.nl/reference/chaptr06/stack/cdmastck.htm*

Liu, D., Wang, Z., Tan, J., Min, H. & Wang, J. (2009). ALOHA algorithm considering the slot duration difference in RFID system, *RFID, 2009 IEEE International Conference on*, pp. 56 –63.

Liu, H. & Guo, X. (2008). A passive UHF RFID system with Huffman sequence spreading backscatter signals, *Proceedings of the 1st international conference on The internet of things*, Springer-Verlag, pp. 184–195.

Liu, Q., Yang, E.-H. & Zhang, Z. (2001). Throughput analysis of CDMA systems using multiuser receivers, *Communications, IEEE Transactions on* 49(7): 1192 –1202.

Liu, Z. & El Zarki, M. (1994). Performance analysis of DS-CDMA with slotted ALOHA random access for packet PCNs, *Personal, Indoor and Mobile Radio Communications, 1994. Wireless Networks - Catching the Mobile Future., 5th IEEE International Symposium on*, Vol. 4, pp. 1034 –1039 vol.4.

Lo, F. L., Ng, T. S. & Yuk, T. (1996). Performance analysis of a fully-connected, full-duplex CDMA ALOHA network with channel sensing and collision detection, *Selected Areas in Communications, IEEE Journal on* 14(9): 1708 –1716.

Loeffler, A., Schuh, F. & Gerhaeuser, H. (2010). Realization of a CDMA-based RFID System Using a Semi-active UHF Transponder, *Wireless and Mobile Communications (ICWMC), 2010 6th International Conference on*, pp. 5 –10.

Maguire, Y. & Pappu, R. (2009). An Optimal Q-Algorithm for the ISO 18000-6C RFID Protocol, *Automation Science and Engineering, IEEE Transactions on* 6(1): 16 –24.

Makwimanloy, S., Kovintavewat, P., Ketprom, U. & Tantibundhit, C. (2009). A novel anti-collision algorithm for high-density RFID tags, *Electrical Engineering/Electronics, Computer, Telecommunications and Information Technology, 2009. ECTI-CON 2009. 6th International Conference on*, Vol. 02, pp. 848 –851.

Mutti, C. & Floerkemeier, C. (2008). CDMA-based RFID Systems in Dense Scenarios: Concepts and Challenges, *RFID, 2008 IEEE International Conference on*, pp. 215–222.

Nikitin, P. & Rao, K. (2008). Antennas and propagation in uhf rfid systems, *RFID, 2008 IEEE International Conference on*, pp. 277 –288.

Pardo, D., Vaz, A., Gil, S., Gomez, J., Ubarretxena, A., Puente, D., Morales-Ramos, R., Garcia-Alonso, A. & Berenguer, R. (2007). Design criteria for full passive long range uhf rfid sensor for human body temperature monitoring, *RFID, 2007. IEEE International Conference on*, pp. 141–148.

Penttila, K., Keskilammi, M., Sydanheimo, L. & Kivikoski, M. (2006). Radar cross-section analysis for passive RFID systems, *Microwaves, Antennas and Propagation, IEE Proceedings* - 153(1): 103 – 109.

Pupunwiwat, P. & Stantic, B. (2010). A RFID Explicit Tag Estimation Scheme for Dynamic Framed-Slot ALOHA Anti-Collision, *Wireless Communications Networking and Mobile Computing (WiCOM), 2010 6th International Conference on*, pp. 1 –4.

Rembold, B. (2009). Optimum modulation efficiency and sideband backscatter power response of RFID-tags, *Frequenz - Journal of RF-Engineering and Telecommunications* 63(1 -2): 9 –13.

Roberts, L. G. (1975). ALOHA packet system with and without slots and capture, *SIGCOMM Comput. Commun. Rev.* 5: 28–42.
URL: *http://doi.acm.org/10.1145/1024916.1024920*

Sakata, A., Yamazato, T., Okada, H. & KATAYAMAt, M. (2007). Throughput Comparison of CSMA and CDMA slotted ALOHA in Inter-Vehicle Communication, *Telecommunications, 2007. ITST '07. 7th International Conference on ITS*, pp. 1 –6.

Sastry, A. (1984). Effect of Acknowledgment Traffic on the Performance of Slotted ALOHA-Code Division Multiple Access Systems, *Communications, IEEE Transactions on* 32(11): 1219 – 1222.

van Nee, R., van Wolfswinkel, R. & Prasad, R. (1995). Slotted ALOHA and code division multiple access techniques for land-mobile satellite personal communications, *Selected Areas in Communications, IEEE Journal on* 13(2): 382 –388.

Wang, L.-C. & Liu, H.-C. (2006). A Novel Anti-Collision Algorithm for EPC Gen2 RFID Systems, *Wireless Communication Systems, 2006. ISWCS '06. 3rd International Symposium on*, pp. 761 –765.

Zhang, Z., Lu, Z., Pang, Z., Yan, X., Chen, Q. & Zheng, L.-R. (2010). A Low Delay Multiple Reader Passive RFID System Using Orthogonal TH-PPM IR-UWB, *Computer Communications and Networks (ICCCN), 2010 Proceedings of 19th International Conference on*, pp. 1 –6.

Current Trends and Challenges in RFID

Edited by Prof. Cornel Turcu

ISBN 978-953-307-356-9
Hard cover, 502 pages
Publisher InTech
Published online 20, July, 2011
Published in print edition July, 2011

With the increased adoption of RFID (Radio Frequency Identification) across multiple industries, new research opportunities have arisen among many academic and engineering communities who are currently interested in maximizing the practice potential of this technology and in minimizing all its potential risks. Aiming at providing an outstanding survey of recent advances in RFID technology, this book brings together interesting research results and innovative ideas from scholars and researchers worldwide. Current Trends and Challenges in RFID offers important insights into: RF/RFID Background, RFID Tag/Antennas, RFID Readers, RFID Protocols and Algorithms, RFID Applications and Solutions. Comprehensive enough, the present book is invaluable to engineers, scholars, graduate students, industrial and technology insiders, as well as engineering and technology aficionados.

How to reference

In order to correctly reference this scholarly work, feel free to copy and paste the following:

Andreas Loeffler (2011). Using CDMA as Anti-Collision Method for RFID - Research & Applications, Current Trends and Challenges in RFID, Prof. Cornel Turcu (Ed.), ISBN: 978-953-307-356-9, InTech, Available from: http://www.intechopen.com/books/current-trends-and-challenges-in-rfid/using-cdma-as-anti-collision-method-for-rfid-research-applications

INTECH
open science | open minds

InTech Europe
University Campus STeP Ri
Slavka Krautzeka 83/A
51000 Rijeka, Croatia
Phone: +385 (51) 770 447
Fax: +385 (51) 686 166
www.intechopen.com

InTech China
Unit 405, Office Block, Hotel Equatorial Shanghai
No.65, Yan An Road (West), Shanghai, 200040, China
中国上海市延安西路65号上海国际贵都大饭店办公楼405单元
Phone: +86-21-62489820
Fax: +86-21-62489821

IntechOpen